

# Silicon-on-insulator tunable waveguide-coupled microdisk resonators with selectively integrated p-i-n diodes

Linjie Zhou and Andrew W. Poon

Department of Electrical and Electronic Engineering, The Hong Kong University of Science and Technology,

Clear Water Bay, Hong Kong SAR, China

Tel: (852)-2358-7905; Fax: (852)-2358-1485; Email: [eeawpoon@ust.hk](mailto:eeawpoon@ust.hk)

**Abstract:** We report a design and analysis of compact silicon-on-insulator tunable waveguide-coupled microdisk resonators with selectively integrated p-i-n diodes. Our simulations suggest that singlemode resonances can be coupled and blueshifted by free-carrier plasma dispersion effect.

©2005 Optical Society of America

**OCIS codes:** (230.5750) Resonators; (230.2090) Electro-optical devices

Silicon-based active devices such as tunable filters, switches and modulators using free-carrier plasma dispersion effect have long been attracting considerable research interest [1]. However, typical refractive index change  $\Delta n$  demonstrated is only in the order of  $10^{-3}$ , which imposes relatively long mm- to cm-sized phase-shifters in conventional Mach-Zehnder interferometer designs [1,2]. In order to attain compact active silicon devices that are sensitive to small  $\Delta n$ , Barrios *et al.* recently proposed and demonstrated compact silicon-on-insulator (SOI) tunable Fabry-Perot microresonators using Bragg mirrors with laterally integrated p-i-n diodes [3].

In this summary, we propose and analyze compact SOI tunable laterally waveguide-coupled microdisk resonators with selectively integrated lateral p-i-n diodes. We also report initial experimental results of SOI passive laterally waveguide-coupled microdisk resonators as a necessary step towards active SOI microdisk devices.

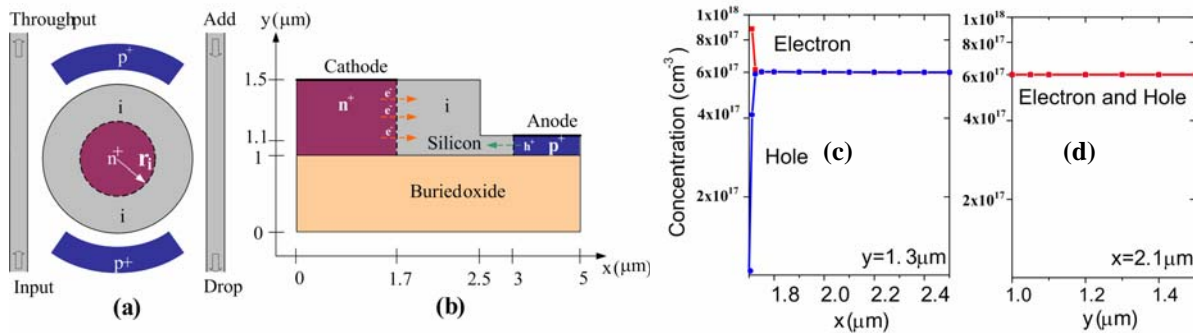


Fig.1. (a) Schematic of a SOI waveguide-coupled microdisk resonator with selectively integrated lateral p-i-n diodes as a tunable channel add-drop filter. (b) Schematic cross-section of the lateral p-i-n diode (under forward bias). (c) Horizontal distributions of free-carriers concentration along  $y=1.3 \mu\text{m}$  in the intrinsic region. (d) Vertical distributions of free-carriers concentration along  $x=2.1 \mu\text{m}$  in the intrinsic region.

Figure 1 (a) shows the schematic of an active microdisk resonator side-coupled with submicrometer single-mode input and output-coupled waveguides. We use lateral p-i-n diodes with n<sup>+</sup>-doped region in the microdisk central region and p<sup>+</sup>-doped region outside the microdisk rim. Upon forward bias, free-carriers are

selectively injected into the arc intrinsic region with lateral p-i-n diodes. The arc region refractive index and absorption can then be selectively tuned by means of free-carrier plasma dispersion effect. Doping can be made by implantation in order to precisely control the lateral dopant profiles. Figure 1 (b) shows the schematic cross-sectional view of our lateral p-i-n diode.

We used semiconductor device simulator MEDICI to simulate the free-carriers concentration profiles. We assumed a uniform dopant concentration of  $10^{20} \text{ cm}^{-3}$  for the  $n^+$  region and of  $10^{19} \text{ cm}^{-3}$  for the  $p^+$  region. Figures 1 (c) and 1 (d) show the calculated electron and hole-carrier distributions by applying a forward bias voltage of 0.91 V at  $y = 1.3 \text{ }\mu\text{m}$  and  $x = 2.1 \text{ }\mu\text{m}$  in the intrinsic region. We observed a flat distribution of about  $6 \times 10^{17} \text{ cm}^{-3}$  for both carriers. Using the free-carrier dispersion at a wavelength of 1550 nm [4], we calculated the refractive index change  $\Delta n = -0.002$  and the associated free-carrier absorption coefficient change  $\Delta \alpha = 8.7 \text{ cm}^{-1}$  at the intrinsic region, and a substantial  $\Delta \alpha = 850 \text{ cm}^{-1}$  at the central  $n^+$  region. Hence, by selectively integrating the lateral p-i-n diodes, we achieve two objectives – (i) preferentially inject carriers to the intrinsic rim region to phase-shift the low-order whispering-gallery modes (WGMs), and (ii) suppress the undesirable high-order WGMs by excessive free-carrier absorption in the microdisk central region.

We used two-dimensional finite-difference time-domain (FDTD) simulations to demonstrate the suppression of high-order WGMs by tuning the size of the heavily doped central region. Here we fix the  $n^+$ -concentration at  $10^{20} \text{ cm}^{-3}$ . We simulated a 5- $\mu\text{m}$  diameter microdisk resonator. Figures 2 (a) and 2 (b) show the FDTD simulated transmission spectra with the  $n^+$  disk radius  $r$  of 1.2  $\mu\text{m}$  and 1.7  $\mu\text{m}$ . With an increase in the central  $n^+$  doped area, the low-order mode A is only slightly shifted (with essentially fixed Q and coupling efficiency), whereas the high-order mode B is partially suppressed. Figure 2 (c) shows the simulated steady-state mode-field patterns of modes A' and B' with the  $r = 1.7 \text{ }\mu\text{m}$   $n^+$  doped region.

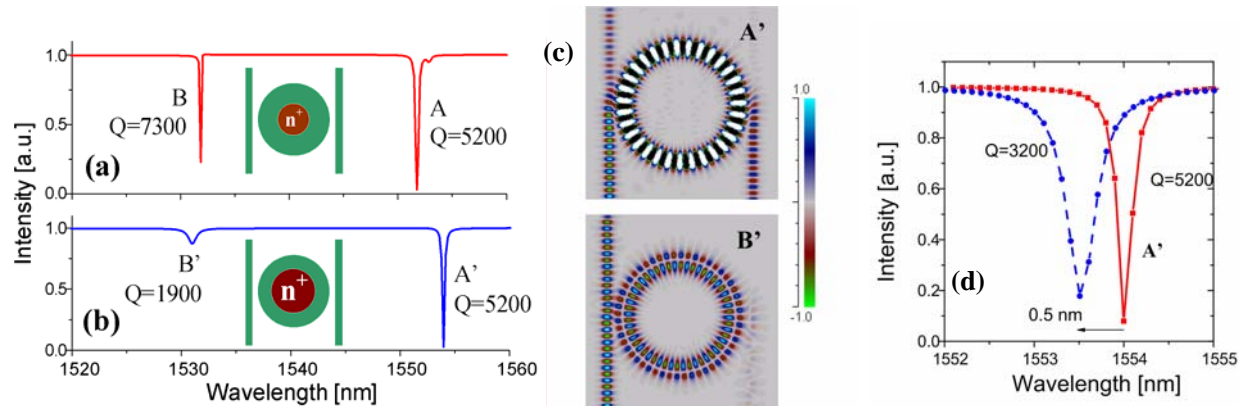


Fig.2. FDTD-simulated transmission spectra at throughput port for 5- $\mu\text{m}$ -diameter microdisk resonators (TM polarized). (a)  $n^+$  doped disk radius  $r = 1.2 \text{ }\mu\text{m}$ , and (b)  $r = 1.7 \text{ }\mu\text{m}$ . We adopted the waveguide refractive index  $n=3.45$ , and the background refractive index of 1.45. (c) Simulated steady-state mode-field patterns of the low-order mode A' and of the partially suppressed high-order mode B'. (d) Simulated mode A' transmission when there is no bias (solid line) and the blueshifted resonance transmission upon a forward biasing of 0.91 V (dashed line).

Figure 2 (d) shows the FDTD-simulated mode A' resonance blueshift of about 0.5 nm upon a forward bias of 0.91 V by imposing a  $\Delta n = -0.002$  and  $\Delta \alpha = 8.7 \text{ cm}^{-1}$  along the arc region with carrier injection. Here we assumed the total active arc length is one-half of the total microdisk circumference (Fig.1(a)). When there is no bias (solid line), the resonance has a  $Q = 5,200$  and a coupling efficiency of about 92 %. Upon forward bias (dashed line), the blueshifted resonance has a reduced  $Q = 3,200$  and a reduced coupling efficiency of about 85 %.

As a necessary step towards active SOI microdisk devices, we demonstrate for the first time to our knowledge SOI passive laterally waveguide-coupled microdisk resonators. We employed standard silicon microfabrication processes. Figure 3 (a) shows the scanning-electron micrograph of our initially fabricated waveguide-coupled 50- $\mu\text{m}$ -diameter passive microdisk resonator on 0.5- $\mu\text{m}$  SOI substrates. Inset shows the cross-sectional view of the side-coupled submicrometer singlemode waveguide with a waveguide height of about 0.35  $\mu\text{m}$  and a width of about 0.35  $\mu\text{m}$ . Figure 3 (b) shows the measured multimode throughput transmission spectrum with TE polarization. Figure 3 (c) shows a zoom-in view of a high-Q mode ( $Q \approx 32,000$ ) with exceeding 16 dB coupling efficiency. This high-Q value is an order of magnitude higher than that recently reported in SOI waveguide-coupled microring resonator [5].

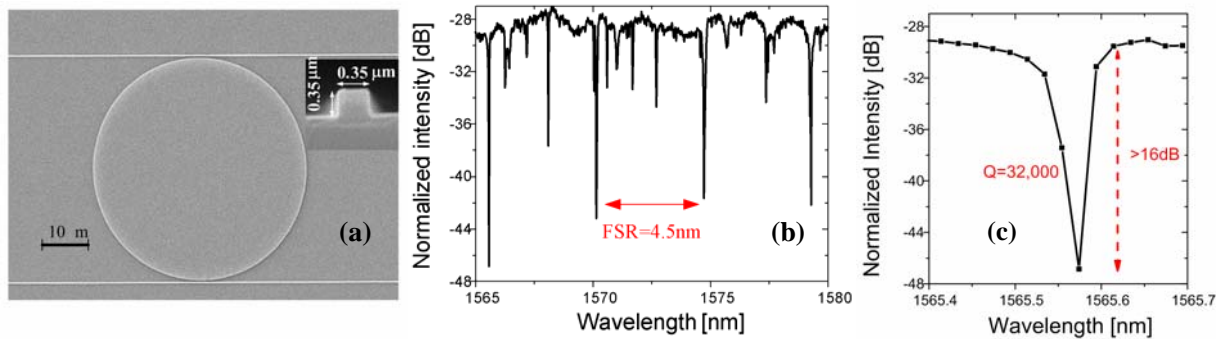


Fig.3. (a) Scanning-electron micrograph of SOI passive waveguide-coupled microdisk resonator on 0.5  $\mu\text{m}$  SOI. Inset shows the cross-sectional view of the submicrometer singlemode waveguide. (b) Measured multimode throughput transmission spectrum with TE polarization. The free-spectral range (FSR) of 4.5 nm is consistent with the microdisk circumference. (c) Zoom-in view shows the high-Q mode with  $Q \approx 32,000$  and a coupling efficiency  $> 16$  dB.

In summary, we report a design and analysis of injection-type active microdisk resonator devices using selectively integrated lateral p-i-n diodes. We took advantage of the large optical absorption loss in the heavily doped microdisk central region in order to suppress undesirable high-order whispering-gallery modes. While the lateral p-i-n diodes selectively inject carriers to phase-shift the low-order whispering-gallery modes along the microdisk rim. Our simulations suggested a resonance wavelength blueshift of about 0.5 nm under a forward bias of only 0.91 V. We also experimentally demonstrated for the first time to our knowledge SOI passive waveguide-coupled microdisk resonators with a high Q of about 32,000 and a high coupling efficiency exceeding 16 dB. Design optimization and fabrication of the proposed SOI active microdisk devices using standard silicon microfabrication processes are in progress.

## References

- [1] G T Reed and A P Knights, *Silicon Photonics: An Introduction* (John Wiley and Sons, 2004).
- [2] A. Liu, R. Jones, L. Liao, D. Samara-Rubio, D. Rubin, O. Cohen, R. Nicolaescu, M. Paniccia, "A high-speed silicon optical modulator based on a metal-oxide-semiconductor capacitor", *Nature* **427**, 615-618 (2004).
- [3] C. Angulo Barrios, V. R. Almeida, R. R. Panepucci, B. S. Schmidt, and M. Lipson, "Compact silicon tunable Fabry-perot resonator with low power consumption", *IEEE Photon. Technol. Lett.* **16**, 506-508 (2004).
- [4] R. A. Soref and B. R. Bennett, "Electrooptical effects in silicon", *IEEE J. Quant. Electron* **23**, 123-129 (1987).
- [5] P. Dumon, W. Bogaerts, V. Wiaux, J. Wouters, S. Beckx, J. V. Campenhout, D. Taillaert, B. Luyssaert, P. Bienstman, D. V. Thourhout, and R. Baets, "Low-loss SOI photonic wires and ring resonators fabricated with deep UV lithography", *IEEE Photon. Technol. Lett.* **16**, 1328-1330 (2004).